

Trajectory-Aware Node Contributions and the Limits of Static Controllability

Valentina V. Kuskova

Lucy Family Institute for Data & Society
University of Notre Dame
Notre Dame, IN, USA
vkuskova@nd.edu

Dmitry Zaytsev

Lucy Family Institute for Data & Society
University of Notre Dame
Notre Dame, IN, USA
zaytsevdi2@gmail.com

Michael Coppedge

Department of Political Science
University of Notre Dame
Notre Dame, IN, USA
mcoppedg@nd.edu

Abstract—A recurring data-mining task in complex, time-evolving networks is to determine how individual nodes contribute to system behavior. Existing approaches rely on either static-graph centralities or control-theoretic quantities such as controllability Gramians, which assume linear, time-invariant dynamics. Estimated systems, however, are typically nonlinear and time-varying. We define *emergent contribution*, a finite-horizon measure of a node’s dynamical leverage: the metric-weighted energy of its impulse response accumulated along the system trajectory. Computed from the Jacobians of any differentiable model, the measure is estimator-agnostic and reduces *exactly* to average controllability in the linear, time-invariant limit.

Our contribution is therefore a characterization of *when* the two measures agree and when they diverge. Using a controlled synthetic family with known ground-truth contribution, we construct a phase diagram spanning nonlinearity, regime structure, persistence, and perturbation amplitude. Emergent contribution and average controllability agree under static or smoothly drifting dynamics and both track ground truth. Divergence emerges under persistent regime switching, is strongest under persistent sign reversal, and disappears when the sign reversal is removed. At extreme perturbation amplitudes, both measures degrade, identifying the limits of local linearization.

We then place five estimated real systems, spanning political, economic, financial, and environmental domains, within this phase space. Their placement serves as a diagnostic of when emergent contribution provides information beyond static controllability and therefore justifies its additional computational cost. On one panel examined in depth, a twenty-seed retraining ensemble reveals a robust variance-leverage dissociation: nodes whose perturbations propagate widely despite low within-system variance, and conversely high-variance nodes whose perturbations do not propagate. This structure is recovered by neither static centralities nor variance-based summaries.

Index Terms—Node contribution, dynamical systems, time-evolving networks, controllability, interpretable modeling, influence, neural vector autoregression, knowledge extraction.

I. INTRODUCTION

A recurring data-mining task in complex, time-evolving systems is to determine which variables are dynamically consequential. Given a multivariate time series and an estimated interaction structure, analysts often wish to identify the components whose perturbations propagate most strongly through the learned system. This problem arises across domains including network neuroscience, systems biology, political economy, economics, and environmental science. In each case, the objective is not merely to recover an interaction network, but

to mine from a fitted dynamical model which variables are most influential for the system’s future evolution.

One line of work approaches this problem through the topology of a static network. Descriptive centralities such as degree, betweenness, closeness, eigenvector centrality, and PageRank measure how a node is positioned within a fixed pattern of connections. These measures remain widely used throughout empirical network science. However, they characterize structural position rather than dynamical influence. A central node is not necessarily one whose perturbations substantially alter the system’s trajectory.

A second line of work treats the network as a dynamical system and evaluates influence through controllability. Structural controllability [1], the controllability Gramian, and the average- and modal-controllability measures of Pasqualetti, Zampieri, and Bullo [2] provide principled node-level summaries of how perturbations propagate through a system. These methods represent a substantial advance over static centralities because they quantify dynamical rather than topological influence. Their interpretation, however, depends on a key assumption: the system is linear and time-invariant, $\dot{x} = Ax + Bu$.

The systems typically estimated from data are neither linear nor time invariant. Their local dynamics depend on the state, and their governing relationships may drift over time. Neural vector autoregressions, nonlinear state-space models, neural ordinary differential equations, and related estimators routinely operate in this regime. Yet controllability-based quantities remain widely used as if the linear time-invariant approximation were sufficient. This raises a fundamental data-mining question: *when do the node rankings implied by static controllability remain reliable, and when do they fail?*

Answering that question requires a node-level measure that remains meaningful for empirically estimated nonlinear, time-varying systems. We therefore define *emergent contribution* E_j , a finite-horizon measure of a node’s dynamical leverage in an estimated dynamical system. The measure is constructed from the state-transition matrix obtained by propagating the system’s Jacobians along its trajectory and requires only that the underlying estimator be differentiable. It therefore applies to graphical and neural vector autoregressions, neural ordinary differential equations, and state-space models alike. The

underlying mathematical object itself, finite-horizon impulse-response energy along a Jacobian-product trajectory, is not new (Section IV-C). Our contribution is its formalization as an interpretable, estimator-agnostic, and gauge-explicit node-level measure for empirically estimated nonlinear, time-varying systems.

The framework contributes four elements needed to study node-level contribution in learned dynamical systems. First, emergent contribution reduces exactly to average controllability in the LTI limit (Section VI). Second, it enables a controlled characterization of when that approximation fails through a synthetic phase diagram (Section IX). Third, it resolves practical issues required for application to learned models, including gauge choice, companion-form lag handling, horizon selection, and estimator-agnostic computation. Fourth, we evaluate the framework across five empirical systems spanning political, economic, financial, and environmental domains (Section X); the resulting placements within the synthetic phase space serve as system-level diagnostics for when the measure provides information beyond static controllability. Throughout, we distinguish dynamical leverage from broader notions of importance. Emergent contribution quantifies how strongly perturbations to a component propagate through an estimated system. It does not imply that a high-leverage component is inherently more valuable, fundamental, or important in a normative sense. Such claims require additional domain-specific arguments. Our focus here is solely on the definition, interpretation, and behavior of the measure itself.

II. RELATED WORK

a) Static network measures: A large literature quantifies node importance through graph-theoretic centralities such as degree, strength, betweenness, closeness, eigenvector centrality, and PageRank [3], [4]. These measures summarize a node’s position within a static network and have proved highly useful across domains. In network psychometrics [5], [6], for example, they support the view of psychological constructs as emergent properties of systems of interacting components. Their limitation for the present problem is fundamental: they characterize topology rather than dynamics. Two systems with identical adjacency structures but different dynamical laws have identical centralities, even though a node may strongly influence one system while having little effect in the other. Related critiques of cross-sectional network analysis have shown that node-level summaries can conflate dynamical influence with latent-variable structure [7], motivating a shift from topological importance to dynamical influence.

b) Controllability-based measures: A second line of work evaluates node influence through the lens of dynamical systems and control theory. Structural controllability [1] studies whether a system can be driven to desired states through inputs at selected nodes, while the controllability Gramian quantifies the energy required to do so. Per-node summaries such as average controllability and modal controllability [2] provide principled measures of dynamical influence and have become widely used in network neuroscience [8]. These

measures move beyond topology by explicitly accounting for system dynamics. Their interpretation, however, rests on the assumption of a linear time-invariant system. When dynamics are nonlinear or vary over time, the fixed matrix A underlying Gramian-based analysis no longer exists, and the standard controllability framework no longer applies directly.

c) Node influence in learned dynamical systems: The challenge is particularly acute for modern data-mining workflows, where dynamical systems are increasingly estimated using flexible nonlinear models. Neural ordinary differential equations [9], neural Granger-causal vector autoregressions [10], [11], and related architectures routinely produce state-dependent, time-varying dynamics. Yet the tools used to interpret node importance in such models often remain either graph-theoretic centralities or controllability measures applied under a linear approximation. As a result, there is no widely used operational measure of node-level contribution that is simultaneously finite-horizon, applicable to empirically estimated nonlinear systems, and directly computable from a fitted model.

Our approach addresses this gap by defining a trajectory-based measure of node-level dynamical leverage that depends only on the Jacobians of the estimated system. The measure reduces exactly to average controllability in the linear time-invariant limit while remaining applicable to nonlinear and time-varying dynamics. Because it is formulated entirely in terms of the estimated Jacobians, it is agnostic to the choice of underlying dynamical estimator and can be applied wherever differentiable system dynamics are available.

d) Relation to nonlinear and operator-theoretic control: Controllability of nonlinear systems is a mature area of control theory, typically studied through Lie-algebraic reachability conditions or empirical and finite-horizon controllability Gramians for nonlinear systems [12]. Operator-theoretic approaches, most notably the Koopman framework, represent nonlinear dynamics through a linear evolution in a lifted observable space and are often paired with data-driven approximations such as dynamic mode decomposition [13]. Our objective is narrower and more operational. Rather than performing a full nonlinear controllability analysis, we seek a finite-horizon, *per-node* scalar that can be computed directly from a fitted model’s Jacobians and that reduces exactly to the average-controllability Gramian trace in the linear limit. While empirical Gramians integrate responses to explicit inputs and Koopman methods seek a global linearizing representation, emergent contribution propagates local Jacobians along the realized trajectory and accumulates the resulting impulse-response energy node by node. The result is a lightweight, estimator-agnostic summary of dynamical leverage rather than a reachability certificate.

e) Relation to sensitivity and attribution methods: Emergent contribution is related to trajectory-sensitivity analysis [14] and to gradient-based attribution methods such as saliency, integrated gradients [15], and neural Granger-causal attribution [10]. Where integrated gradients accumulate gradients along a path in *input* space to attribute a single prediction,

emergent contribution propagates perturbations through the full state-transition operator along a path in *time*, accumulating influence over a declared horizon. Its exact reduction to average controllability in the LTI limit additionally provides a control-theoretic interpretation unavailable to purely attribution-based measures.

f) Influence and spreading on networks: A separate literature studies a node’s capacity to spread influence through a network, including independent-cascade and linear-threshold models and the influence-maximization problem they motivate [16]. Like emergent contribution, these approaches quantify propagation. The difference is that they operate on a prescribed stochastic diffusion process over a fixed graph, whereas emergent contribution propagates the *estimated* deterministic dynamics of a fitted multivariate system and therefore inherits its nonlinearity and time variation. The two perspectives are complementary: one studies spreading behavior under an assumed contagion process, while the other measures dynamical leverage in a learned dynamical system.

We are particularly motivated by settings in which system-level behavior is viewed as emerging from interactions among constituent components, as in network psychometrics [5], [6]. Our contribution is not a new static centrality, but a dynamical measure of node-level contribution for nonlinear and time-varying systems. In this sense, the framework extends existing approaches to node importance by providing an operational notion of contribution in precisely the settings where classical controllability theory no longer applies directly.

III. SETUP AND NOTATION

Consider a discrete-time dynamical system on n components. After collapsing any finite lag structure into companion form, write the one-step map as

$$x_{t+1} = f_t(x_t) + \varepsilon_t, \quad x_t \in \mathbb{R}^n. \quad (1)$$

The map f_t may be **nonlinear** and may depend on t (**time-varying**); ε_t is mean-zero noise. The local causal influence of the components on one another is the Jacobian of the map evaluated along the realized trajectory,

$$A_t(x) = \left. \frac{\partial f_t}{\partial x} \right|_x \in \mathbb{R}^{n \times n}, \quad (2)$$

whose (i, j) entry is the marginal effect of component j at time t on component i at time $t + 1$, given the current state x .

Multi-step propagation is governed by the **state-transition matrix**, the ordered product of Jacobians along the trajectory:

$$\Phi_t^\tau(x) = A_{t+\tau-1}(x_{t+\tau-1}) \cdots A_{t+1}(x_{t+1}) A_t(x_t), \quad (3)$$

with $\Phi_t^0(x) = I$ and the trajectory generated by $x_t = x$ and $x_{s+1} = f_s(x_s)$. The j -th column, $\Phi_t^\tau(x) e_j$, is the **local impulse response**: the location of a small perturbation to component j at time t after τ steps of propagation. Because the product is evaluated along the realized trajectory, it captures both nonlinearity (through state-dependent Jacobians) and time variation (through changes in the Jacobians across time). The state-transition matrix is the fundamental object underlying

all subsequent definitions. The distinction between simulated and observed trajectories becomes important because the state-transition matrix depends on the sequence of Jacobians along which it is evaluated.

a) Choice of trajectory: The definition above generates the trajectory by iterating the estimated map, $x_{s+1} = f_s(x_s)$, yielding a **model-simulated** trajectory. This choice isolates the intrinsic dynamics implied by the fitted model. In empirical applications, one may instead evaluate Jacobians along the **observed realized** trajectory $\{x_s\}$ from the data, addressing a different question: how leverage propagated along the path the system actually followed rather than along the path predicted by the model. The two coincide under perfect model fit and otherwise differ. We use the simulated trajectory throughout the formal development and theoretical reductions below, and note explicitly whenever an empirical diagnostic substitutes the observed trajectory.

IV. THE CONSTRUCT: EMERGENT CONTRIBUTION

Definition 1 (Emergent contribution). The emergent contribution of component j , at time t , from state x , over horizon T is

$$E_j(t, x; T) = \sum_{\tau=0}^{T-1} (\Phi_t^\tau(x) e_j)^\top M (\Phi_t^\tau(x) e_j), \quad (4)$$

with $\Phi_t^0(x) = I$ and M a fixed positive-definite metric that declares what “system impact” means. The default is $M = I$ on standardized components (see Section V).

a) Interpretation: E_j is the total M -weighted energy of component j ’s impulse response, accumulated over a horizon of length T . Components whose perturbations propagate broadly or persist over time have high emergent contribution, whereas components whose perturbations remain localized or decay rapidly have low contribution.

b) Naming: Outside the LTI limit, E_j is not a controllability measure in the reachability sense of control theory. Rather, it is a finite-horizon measure of dynamical leverage, or equivalently, impulse-response energy accumulated along a trajectory. The quantity can be viewed as a trajectory-level generalization of the average-controllability Gramian trace, with state-dependent Jacobian products $\Phi_t^\tau(x)$ replacing matrix powers A^τ . In the LTI limit, the two coincide exactly (Section VI). Outside that regime, we interpret E_j as finite-horizon dynamical leverage rather than a reachability certificate. Accordingly, we reserve the term ‘average controllability’ for the LTI reduction and use ‘dynamical leverage’ or ‘impulse-response energy’ elsewhere.

c) Finite-horizon by design: E_j is defined for a finite horizon T , and T is a declared parameter rather than a limit to be taken. This matters because systems with spectral radius near or above 1 can exhibit growing impulse-response energy, causing E_j to diverge as $T \rightarrow \infty$. The finite-horizon definition is therefore a modeling choice rather than a technical convenience: E_j measures leverage *accumulated over a stated horizon*, and any reported value must specify T . Comparisons across nodes, states, or times must hold T fixed.

d) *The self-term* ($\tau = 0$) is retained: The $\tau = 0$ term contributes $e_j^\top M e_j$ to E_j and should not be removed. For $M = I$, it equals 1 for every node, but subtracting a constant from every node does *not* preserve the normalized weights of Section IV-A, because normalization is not shift-invariant. Accordingly, the self-term is retained; one should not “exclude the diagonal.”

A. From leverage to weights (an optional aggregation)

If one wishes to aggregate components into a single score - a step requiring a separate, domain-specific normative argument that we do not make here - the contribution induces aggregation weights

$$w_j(t, x) = \frac{E_j(t, x; T)}{\sum_k E_k(t, x; T)}. \quad (5)$$

These weights are **state-dependent and time-dependent by construction**. This dependence is intentional: a component’s contribution to system dynamics depends on the regime the system occupies and on how the dynamics have evolved. Throughout, we use these weights only as a normalized reporting device for relative leverage, not as a normative aggregation.

B. What E_j measures, and what it does not

E_j measures the **dynamical leverage** of component j in the *estimated* system: the extent to which perturbations to j propagate through the system’s dynamics. By itself, it does **not** establish that j is more important, more valuable, or more fundamental than other components. High leverage is compatible with at least three distinct interpretations:

- (a) a **load-bearing** component on which system behavior depends;
- (b) a **fragile amplifier** that transmits shocks destructively; or
- (c) a **highly endogenous relay** that primarily propagates the behavior of other components.

The statement that “component j has dynamical leverage E_j in the estimated system” is descriptive and carries no normative implication. Any claim that leverage should determine importance - for example, that an aggregate score ought to weight components by leverage - requires a separate, domain-specific justification that lies outside the scope of this paper. Throughout, we interpret E_j as a measure of dynamical leverage rather than a normative measure of importance.

C. Impulse-response energy and the contribution

Mathematically, E_j is finite-horizon impulse-response energy accumulated along a trajectory. The novelty therefore lies not in a new dynamical quantity, but in its formalization as an operational node-level measure for empirically estimated systems. The remainder of the paper establishes its exact reduction to average controllability in the linear time-invariant limit (Section VI), addresses the practical issues required for computation on learned dynamical models (Sections V–VIII), and characterizes the conditions under which it departs from static controllability (Sections IX–X).

Algorithm 1 Computation of emergent contribution

Require: fitted differentiable model f ; trajectory x_t, \dots, x_{t+T-1} ; horizon T ; metric M ; lag order K

Ensure: emergent contributions $\{E_j\}_{j=1}^n$ and weights $\{w_j\}$

- 1: **if** $K > 1$ **then** construct companion coordinates; state dimension $d \leftarrow nK$
- 2: **else** $d \leftarrow n$
- 3: **end if**
- 4: **for** $s = 0, \dots, T - 2$ **do**
- 5: $A_s \leftarrow$ Jacobian of f at x_{t+s} \triangleright autodiff; companion if $K > 1$
- 6: **end for**
- 7: **for** $j = 1, \dots, n$ **do**
- 8: $v \leftarrow e_j^{(0)}$ \triangleright perturb node j in current-state block
- 9: $E_j \leftarrow v^\top M v$ $\triangleright \tau = 0$ self-term, retained
- 10: **for** $\tau = 1, \dots, T - 1$ **do**
- 11: $v \leftarrow A_{\tau-1} v$ \triangleright propagate: $v = \Phi^\tau e_j^{(0)}$
- 12: $E_j \leftarrow E_j + v^\top M v$
- 13: **end for**
- 14: **end for**
- 15: $w_j \leftarrow E_j / \sum_k E_k$ \triangleright normalized leverage weights
- 16: **return** $\{E_j\}, \{w_j\}$

D. Algorithm

Algorithm 1 gives the operational computation of emergent contribution. A node-perturbation vector is propagated through the Jacobian sequence via repeated matrix–vector products, accumulating metric-weighted energy at each step, including the $\tau = 0$ self-term.

E. Computational complexity

Let d denote the state dimension ($d = n$ for $K = 1$ and $d = nK$ in companion coordinates) and T the horizon. Jacobian extraction requires $T - 1$ autodiff evaluations, with cost determined by the model architecture; the additional companion-coordinate blocks come from the same per-lag Jacobian and require no separate evaluations.

Propagation is specific to emergent contribution: each node requires $O(Td^2)$ matrix–vector operations, yielding $O(nTd^2) = O(n^3K^2T)$ overall in companion coordinates. This is cheaper than explicitly forming the matrix products Φ^τ , which costs $O(Td^3)$. Memory usage is $O(d^2)$ for the current Jacobian plus $O(d)$ per propagated vector. Once Jacobians are available, the remaining cost is matrix–vector products and is typically inexpensive relative to model fitting.

V. SCALE DEPENDENCE AND THE GAUGE CHOICE

Scale dependence is a fundamental property of E_j , not a secondary implementation detail. Because E_j is defined as a squared M -norm of impulse responses, both its value and the induced weights depend on the units of the components, their standardization, and the choice of coordinates. Numerically, rescaling components by a diagonal matrix D while holding $M = I$ fixed can shift a single node’s weight share across

most of its possible range, from a small minority to a large majority of the total. Consequently, any interpretation of E_j requires an explicit choice of coordinate system and metric.

a) *The gauge:* Our default choice is to compute E_j on **standardized components** (each component centered and scaled to unit variance) with $M = I$, and to define “system impact” in standardized-component units. This is a modeling choice and must be stated explicitly. It is also the natural default, because it places all components on a common scale before measuring how perturbations propagate through the system.

b) *Coordinate transformation law:* Under a linear change of coordinates $x' = Dx$, the dynamics transform as $A' = DAD^{-1}$ and the impulse responses as $\Phi' = D\Phi D^{-1}$. The contribution remains invariant if and only if the metric transforms according to $M' = D^{-\top}MD^{-1}$. Declaring the standardized metric $M = I$ in standardized coordinates therefore fixes the gauge. Any reported value of E_j is understood relative to that declared metric.

VI. MAIN RESULT: REDUCTION TO AVERAGE CONTROLLABILITY IN THE LTI LIMIT

The key theoretical property of emergent contribution is that it reduces *exactly* to the average controllability measure of Pasqualetti, Zampieri, and Bullo [2] in the linear time-invariant (LTI) limit. The measure therefore extends a well-established quantity rather than introducing an unrelated notion of node influence.

Proposition 1 (LTI-limit reduction). *Suppose $f_t(x) = Ax$ for a constant matrix A (the LTI limit), take $M = I$, and use Definition (4) (sum $\tau = 0, \dots, T-1$, $\Phi^0 = I$). Then*

$$E_j(t, x; T) = \text{AC}_j(T) = \text{tr } W_j(T), \quad (6)$$

independent of t and x , where

$$W_j(T) = \sum_{\tau=0}^{T-1} A^\tau e_j e_j^\top (A^\top)^\tau \quad (7)$$

is the node- j average-controllability Gramian.

Proof. In the LTI limit the Jacobian is constant, $A_t(x) = A$, so the state-transition matrix is a matrix power, $\Phi_t^\tau(x) = A^\tau$, with $A^0 = I$. Hence, taking $M = I$,

$$\begin{aligned} E_j(t, x; T) &= \sum_{\tau=0}^{T-1} \|A^\tau e_j\|^2 \\ &= \sum_{\tau=0}^{T-1} e_j^\top (A^\top)^\tau A^\tau e_j \\ &= \sum_{\tau=0}^{T-1} \text{tr}(A^\tau e_j e_j^\top (A^\top)^\tau) \quad (\text{cyclic property of trace}) \\ &= \text{tr} \sum_{\tau=0}^{T-1} A^\tau e_j e_j^\top (A^\top)^\tau \\ &= \text{tr } W_j(T) = \text{AC}_j(T). \end{aligned}$$

Remark (Indexing convention). The reduction requires the sum in Definition (4) to run over $\tau = 0, \dots, T-1$ with the $\Phi^0 = I$ term included. Using instead $\tau = 1, \dots, T$ yields $\text{tr } W_j(T+1) - (e_j^\top M e_j)$, which both adds the A^T term and removes the $A^0 = I$ term. This difference is not merely a uniform shift: because the weights of Section IV-A are obtained by normalization, changing the indexing alters the resulting weights.

a) *Continuous-time version:* The same reduction holds in continuous time. In the LTI limit, $\Phi(\tau) = e^{A\tau}$, giving

$$E_j = \int_0^T \|e^{A\tau} e_j\|^2 d\tau = \text{tr} \int_0^T e^{A\tau} e_j e_j^\top e^{A^\top \tau} d\tau, \quad (8)$$

which is precisely the trace of the finite-horizon continuous-time controllability Gramian. The discrete-time expression is exactly the finite-horizon discrete Gramian trace; its correspondence with the continuous-time form arises through the usual discretization limit rather than through direct equality at finite step size.

VII. WHEN EMERGENT CONTRIBUTION DIFFERS FROM AVERAGE CONTROLLABILITY

The exact reduction of Section VI establishes that emergent contribution recovers average controllability whenever the assumptions of the linear time-invariant model hold. The central question is therefore not whether E_j differs from average controllability, but under what conditions the two begin to diverge.

a) *Nonlinearity:* When f_t is nonlinear, the state-transition matrix $\Phi_t^\tau(x)$ is formed from *state-dependent* Jacobians rather than powers of a fixed matrix. Consequently, E_j becomes state-dependent: a node’s dynamical leverage may vary across operating regimes even when the underlying network structure remains unchanged.

Nonlinearity alone is not the primary source of divergence from average controllability. Across the synthetic systems studied in Section IX-A, purely nonlinear but otherwise stable dynamics produce rankings that remain close to those implied by average controllability. The substantial departures arise instead when nonlinearity interacts with persistent regime structure, causing the realized Jacobian products to differ systematically from powers of their average. Under those conditions, the rank correlation between emergent contribution and average controllability declines substantially and node orderings are reorganized. The generalization is therefore non-trivial, but for a specific and identifiable reason rather than because nonlinearity alone is present.

b) *When E_j departs from average controllability:* The practical question is when emergent contribution changes the answer rather than reproducing the familiar controllability ranking. The decomposition provides the underlying mechanism. Average controllability replaces the realized sequence of Jacobian products with powers of an average Jacobian, \bar{A} . The two measures therefore agree when the realized products \square remain close to powers of \bar{A} , and diverge when they do not.

Sign reversal provides a sufficient mechanism for departure that is transparent enough to analyze directly. Suppose a pathway propagates perturbations positively in one regime and negatively in another. Averaging the Jacobians causes these opposing effects to cancel, making the corresponding entry of \bar{A} appear weak. Emergent contribution, by contrast, accumulates propagation along the realized trajectory and therefore retains the contribution associated with each regime. The result is a discrepancy between the node’s realized contribution and its controllability ranking under the averaged system.

Sign reversal is not the only mechanism that can produce divergence, nor do we claim that it explains any particular empirical system. Instead, Section IX-A characterizes the phenomenon against known ground truth using a controlled sweep of nonlinearity, regime structure, persistence, and perturbation amplitude. Across these experiments, departures from average controllability are negligible for static and smoothly drifting dynamics, emerge under persistent regime change, and become strongest when persistent sign reversal interacts with nonlinearity. At sufficiently large perturbation amplitudes, however, the local-linearization approximation underlying E_j itself begins to degrade.

The resulting conclusion is deliberately bounded. Emergent contribution is most informative when the estimated dynamics exhibit persistent regime-dependent variation while remaining within an operating range for which local linearization remains faithful.

c) Time-variation: When f_t varies over time, the state-transition matrix combines Jacobians drawn from different dynamical regimes. As a result, E_j becomes explicitly time-dependent, tracking how node-level dynamical leverage changes as the estimated system evolves.

d) Scope of the novelty: The novelty of emergent contribution does not lie in introducing nonlinear or time-varying controllability theory, both of which are well established within control theory. Rather, it lies in providing an **operational, finite-horizon measure of node-level contribution for empirically estimated nonlinear, time-varying systems**. This is the setting encountered in many applications of network neuroscience and empirical network science, where average controllability is typically computed under the linear time-invariant approximation. Emergent contribution fills this operational gap: it is computable from estimated Jacobians, reduces exactly to average controllability in the LTI limit, and remains meaningful when the underlying dynamics are nonlinear, time-varying, or regime-dependent.

VIII. ESTIMATOR-AGNOSTICISM AND UNCERTAINTY

a) Estimator-agnostic: E_j requires only the Jacobians $A_t(x)$ evaluated along a trajectory. Any differentiable dynamical model supplies them, including graphical or neural VARs, neural ODEs, and state-space models. In the application below, the Jacobians are obtained from a neural Granger-causal vector-autoregressive model, but the definition of E_j does not depend on that choice. Changing the estimator changes the Jacobians supplied to the measure, not the measure itself. The

contribution is therefore the *measure*: a procedure for extracting node-level dynamical leverage from a fitted dynamical model, with the estimator serving as a replaceable source of Jacobians.

b) The companion operator: For a model with K lags, the Jacobian used for E_j (and for any stability analysis) should be the $(nK \times nK)$ **companion** Jacobian, whose eigenvalues are the true multipliers of the K -lag system. The leading lag-1 block alone is not the correct multi-step propagation operator because it omits the contribution of longer lags to system dynamics. Using the companion form ensures that the state-transition product Φ_t^τ correctly represents propagation when $K > 1$.

c) What “perturbing node j ” means in companion coordinates.: In companion form, the lifted state stacks the current and lagged components, $z_t = (x_t, x_{t-1}, \dots, x_{t-K+1}) \in \mathbb{R}^{nK}$. A perturbation to node j is applied to the current-state block only. The perturbation vector $e_j^{(0)} \in \mathbb{R}^{nK}$ equals 1 in the j -th position of the leading (x_t) block and 0 elsewhere, including all lagged copies of j . Perturbing every lagged copy simultaneously corresponds to a different input and does not represent a perturbation to node j at time t . Accordingly, in companion coordinates, E_j uses $e_j^{(0)}$ in place of e_j throughout Definition (4). The state-transition operator Φ_t^τ then propagates that current-state perturbation into the lagged blocks at later times according to the system dynamics, making the node definition unambiguous for $K > 1$.

d) Uncertainty propagation: Because E_j is a functional of estimated Jacobians, it inherits uncertainty from the underlying dynamical model. In empirical applications, uncertainty should therefore be quantified through an explicit resampling or ensemble procedure rather than reported solely as a point estimate. The choice of resampling scheme determines which sources of uncertainty are captured. **Resampling units** (here, countries as the natural cluster in a country panel) capture sampling uncertainty over the population of units; **block bootstrapping in time** captures uncertainty arising from temporal dependence; **resampling residuals** capture innovation uncertainty conditional on the fitted dynamics; and **re-running the estimator with different random seeds** captures optimization stochasticity. Each procedure induces a distribution over the contributions E_j and the corresponding weights w_j . For the panel studied here, a natural default is a country (cluster) bootstrap, optionally combined with a seed ensemble to distinguish sampling variability from estimation variability. The resulting uncertainty is a computed quantity whose interpretation depends on the chosen resampling scheme.

e) Time aggregation: When a single per-unit score is desired, one must specify where the state-dependent quantity E_j is evaluated: at the current state, averaged along a trajectory, or at a basin equilibrium. Each choice yields a different summary of dynamical leverage and may be appropriate in different applications. Accordingly, the aggregation scheme should be stated explicitly and justified in context.

IX. SYNTHETIC VALIDATION

We validate emergent contribution in two stages: a simple planted system that illustrates the departure from average controllability, followed by a controlled phase diagram that characterizes when that departure occurs across a broader space of dynamics.

a) A warm-up: We begin with a six-node saturating system, $x_{t+1} = \tanh(Wx_t)$. Node 0 is a hub with strong outgoing connections to nodes 1, 2, 3, whereas node 4 contains a saturation-immune self-loop. Near the origin, $A(x) \approx W$ and E_j coincides with the average-controllability Gramian trace to machine precision. As the hub’s pathways saturate, however, its leverage collapses and shifts to node 4 (hub share $0.46 \rightarrow 0.15$, node 4 share $0.14 \rightarrow 0.23$), producing a reordering that average controllability, which depends only on W , cannot capture.

b) Companion-operator ablation: For $K > 1$, the companion operator rather than the lag-1 Jacobian block is the correct propagation operator. On a controlled VAR(2) system with non-trivial lag-2 structure, the lag-1 surrogate not only understates contributions but also *selects the wrong top node* (rank correlation 0.80 relative to the correct companion ordering). The choice therefore affects substantive conclusions rather than merely numerical magnitudes.

c) Sign-cancellation: an isolated departure: We next isolate one mechanism by which E_j can depart from average controllability. The system alternates between two regimes, with occasional transitions between them. One node d acts as a persistent driver, but its downstream pathway reverses sign across regimes while all other edges remain fixed. Within each regime, d is strongly contributive; in the averaged Jacobian, however, the positive and negative pathway contributions cancel, causing average controllability to view the node as weak.

Using a ground-truth contribution computed by propagating perturbations through the true nonlinear dynamics, E_j recovers the node ordering exactly and ranks d first, matching the ground truth. Average controllability, by contrast, misranks d toward the middle because it cannot recover the regime-specific sign structure. A corresponding control experiment removes the sign reversal while leaving the remainder of the construction unchanged. In that setting, the discrepancy disappears entirely. Sign cancellation is therefore a sufficient condition for separation in this controlled example, though not necessarily the only one. The broader space of departures is characterized by the phase diagram that follows.

A. A phase diagram of fidelity to ground truth

The experiments above establish particular instances of departure. We now characterize *when* emergent contribution tracks true contribution, when average controllability suffices, and when both fail. To do so, we generate trajectories from a two-regime nonlinear system,

$$x_{t+1} = A_{r_t} x_t + \alpha \tanh(B_{r_t} x_t) + \varepsilon_t,$$

and systematically vary four factors: *nonlinearity* ($\alpha \in \{\text{low, med, high}\}$); *regime structure* (static, smooth drift, per-

TABLE I
GROUND-TRUTH FIDELITY ADVANTAGE OF E_j OVER POOLED AVERAGE CONTROLLABILITY, BY REGIME STRUCTURE AND NONLINEARITY.

Regime structure	low	med	high
Static	0.01	0.05	0.03
Smooth drift	0.00	-0.01	0.01
Persistent reroute	0.01	0.04	0.10
Sign reversal	0.26	0.47	0.58

sistent reroute, persistent sign reversal); *regime persistence* relative to the evaluation horizon; and *perturbation amplitude* used for the ground-truth probe.

For each cell, we compute three quantities across 20 random seeds: $\rho(E_j, E_{\text{true}})$, $\rho(\text{AC}, E_{\text{true}})$, and $\rho(E_j, \text{AC})$, where E_{true} is obtained by finite-amplitude perturb-and-propagate through the *true* nonlinear dynamics rather than through an estimated model. Average controllability is evaluated under two baselines: a single mean-state linearization (*pooled*) and the average of the realized Jacobians (*realized*).

The primary outcome is fidelity to ground truth rather than the magnitude of the E_j –AC discrepancy itself. A departure is only meaningful if emergent contribution is the measure that more accurately tracks the true contribution.

a) Four regimes: Define $\Delta = \rho(E_j, E_{\text{true}}) - \rho(\text{AC}_{\text{pooled}}, E_{\text{true}})$ as the fidelity advantage of emergent contribution over a single mean-state linearization, with positive values indicating that E_j more closely tracks ground truth. Table I and Figure 1 reveal four distinct operating regimes. The pattern is particularly clear in the seed-level robustness analysis: across 20 seeds, the advantage of E_j is significant in 97% of sign-reversal cells and 56% of persistent-reroute cells, but only 8–17% of static and smooth-drift cells.

(i) Controllability-sufficient. Under static or smoothly drifting dynamics, E_j , both controllability baselines, and ground truth nearly coincide ($\Delta \approx 0$) across all levels of nonlinearity. Smooth drift is an especially informative negative control, showing that time variation alone does not induce separation.

(ii) E_j separates. Under persistent sign reversal at moderate and high nonlinearity, E_j maintains fidelity near 0.93, whereas the pooled baseline falls to approximately 0.35–0.48. The resulting advantage reaches $\Delta = 0.47$ (95% CI [0.32, 0.63]) at medium nonlinearity and $\Delta = 0.58$ ([0.40, 0.77]) at high nonlinearity, with both intervals excluding zero.

(iii) Intermediate. Persistent reroute - a change in the dominant driver without sign reversal - produces a smaller but consistent advantage ($\Delta \leq 0.10$), significant in more than half of the corresponding cells. This indicates that persistent regime change in general can generate separation, with sign reversal representing the strongest case rather than the only one.

(iv) Both fail. At extreme perturbation amplitudes, the local linearization underlying E_j begins to lose fidelity. Under sign reversal, fidelity declines from approximately 0.94 to 0.88 as amplitude increases and converges toward the controllability baselines. This defines the validity boundary of the measure: a

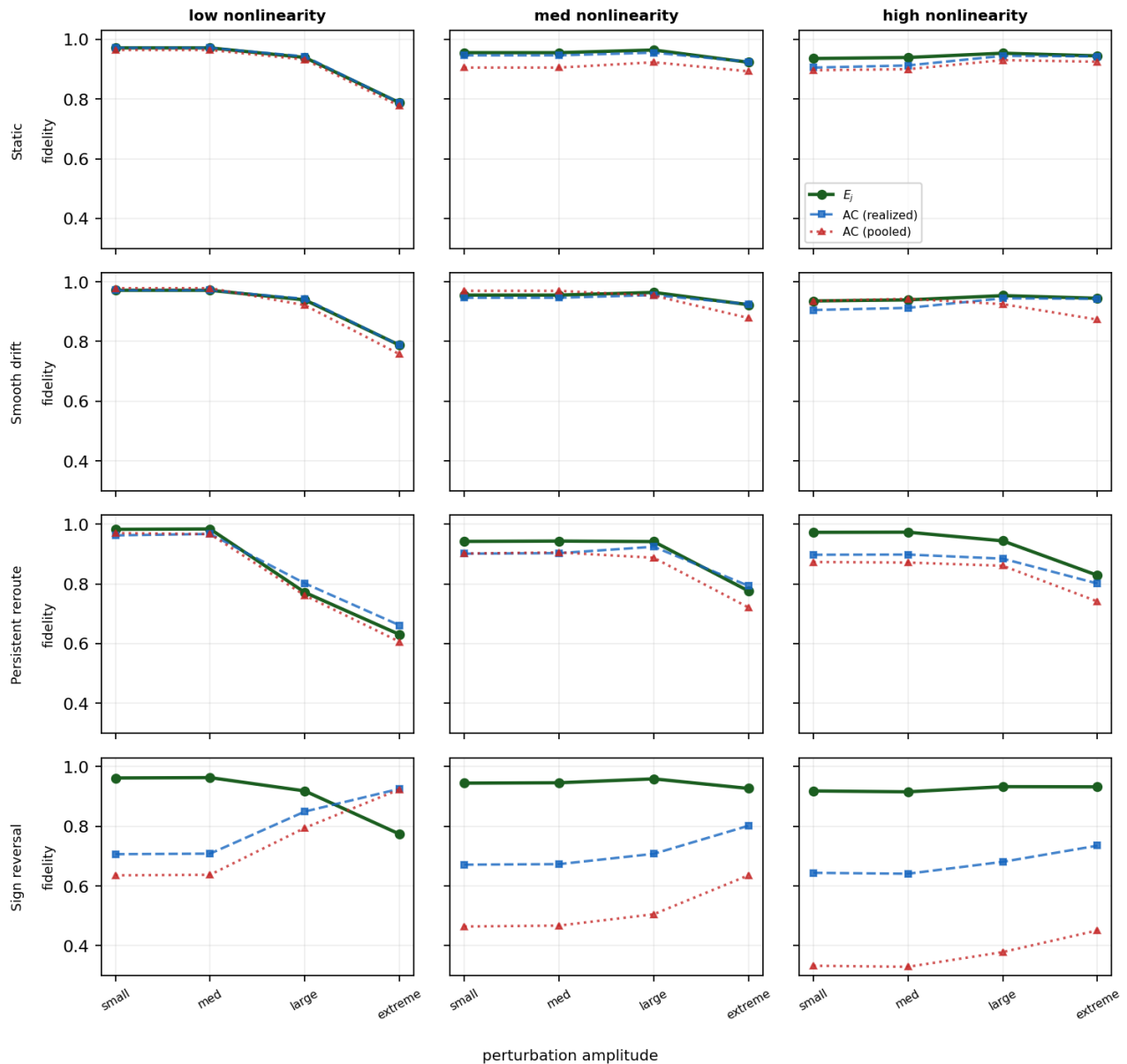


Fig. 1. **Phase diagram: when emergent contribution departs from average controllability.** Each panel reports fidelity to ground-truth contribution (Spearman rank correlation) as perturbation amplitude varies for emergent contribution E_j (solid green), average controllability computed from the average realized Jacobian (dashed blue), and average controllability from a single mean-state linearization (dotted red). Rows correspond to regime structure (top to bottom: static, smooth drift, persistent reroute, persistent regime-dependent sign reversal); columns correspond to nonlinearity (left to right: low, medium, high). Under static and smoothly drifting dynamics, all methods closely track ground truth. Under persistent reroute, E_j exhibits a modest fidelity advantage. Under persistent sign reversal, E_j substantially outperforms both controllability baselines, while the pooled linearization degrades sharply. Shaded regions mark the extreme-amplitude boundary, beyond which the local-linearization approximation underlying E_j begins to lose fidelity and all methods converge.

local-linearization approach cannot faithfully track sufficiently large-amplitude propagation. Consistent with this interpretation, under low nonlinearity and extreme amplitude the pooled baseline can outperform E_j (0.92 versus 0.77). When exploitable nonlinear structure is weak and the perturbation lies outside the faithful regime, E_j has little to gain and its approximation has more to lose.

Together, these four regimes define a practical decision rule, summarized in Table II.

TABLE II
MAIN EMPIRICAL FINDINGS: WHEN TO USE E_j .

Regime structure	E_j vs. AC	Practitioner takeaway
Static / smooth drift	agree	AC suffices
Persistent reroute	E_j ahead	worth checking
Sign reversal	E_j wins	use E_j
Extreme amplitude	both fail	beyond either

b) *A hierarchy of approximations*: Figure 1 supports a secondary but important conclusion: the realized-Jacobian baseline (dashed) consistently outperforms the single mean-state linearization (dotted). Averaging realized Jacobians already recovers much of the trajectory structure discarded by a single linearization. The additional gain provided by E_j comes from preserving the *order* of propagation rather than merely averaging it. The implication is not that static controllability is uninformative, but that there exists a hierarchy of approximations: single linearization, averaged Jacobians, and ordered trajectory products, with E_j occupying the most faithful end of that hierarchy in the regimes identified by the phase diagram.

c) *Exact reduction across horizons*: Across random constant matrices A , system sizes $n \in \{3, 4, 5, 6\}$, and horizons $T \in \{5, 8, 12, 20\}$, the discrepancy $\max_j |E_j - \text{tr } W_j(T)|$ is zero to machine precision, confirming Proposition 1 numerically.

X. PLACING REAL SYSTEMS IN THE PHASE DIAGRAM

The synthetic experiments characterize the measure itself; we now ask where estimated real systems fall within that characterization. Using the same neural vector-autoregressive model (lag three, companion Jacobians, horizon $T = 8$), we analyze five public multivariate panels spanning distinct domains and measure how far the E_j ordering departs from average controllability under the two baselines of Section IX-A.

The democracy panel comprises 16 component indicators from the Varieties of Democracy (V-Dem) project [17], capturing electoral, deliberative, participatory, liberal, and egalitarian dimensions of democracy for 89 countries over 1950–2024. Following a pre-registered temporal split at year 2000, leverage is estimated using the pre-cutoff window (4,094 country-years after lag construction), with post-2000 observations held out. The development panel comprises 8 World Bank World Development Indicators [18]; the macro-finance panel contains 9 macroeconomic series from the Global Macro Database [19]; the realized-volatility panel contains daily realized volatilities for 8 major global equity indices [20]; and the air-quality panel contains 11 pollutant and meteorological variables from multi-site monitoring in Beijing, 2013–2017 [21]. These panels differ substantially in dimensionality, sampling frequency, and underlying substrate by design.

All panels are modeled using the same neural vector-autoregressive architecture, optimization procedure, and training schedule. Full model specification, preprocessing details, train-validation splits, and the frozen synthetic data-generating process are **released in the anonymized reproducibility bundle**.¹

a) *Reading the placement against the stronger baseline*: In Table III, departure is defined as $1 - \rho(E_j, AC)$. We focus on departure from the *realized*-Jacobian baseline because Section IX-A identified it as the stronger controllability approximation: averaging realized Jacobians already recovers much of the trajectory structure discarded by a single linearization.

¹For code and configuration while the paper is under review, please contact the authors.

TABLE III

FIVE ESTIMATED REAL SYSTEMS PLACED IN THE PHASE DIAGRAM. REALIZED DEPARTURES ARE REPORTED AS SEED-ENSEMBLE MEANS \pm S.D., AS THE REAL-DATA GAPS ARE SMALL, SEED-SENSITIVE QUANTITIES (SEE TEXT).

Domain	n	realized	region
Macro-finance	9	0.09 ± 0.04	intermediate
Democracy	16	0.04 ± 0.03	moderate
Economic development	8	0.02 ± 0.01	near-zero
Air quality	11	0.01 ± 0.01	near-zero
Realized volatility	8	0.01 ± 0.01	near-zero

Realized departure is $1 - \rho(E_j, AC^{\text{realized}})$, reported as the mean \pm s.d. over a retraining ensemble (8 seeds; 3 for air quality, 20 for democracy). The gaps are small and seed-sensitive, so we report distributions rather than point estimates. The pooled-baseline comparison is even more variable across seeds and is discussed in the text rather than tabulated.

Viewed through this baseline, the five domains form a gradient consistent with the synthetic characterization. Economic development (0.02), air quality (0.01), and realized volatility (0.01) exhibit essentially no departure, indicating that E_j provides little additional information beyond the realized Jacobian average. This near-zero placement is robust across the retraining ensemble: every seed places all three of these panels at or below 0.03. These systems therefore occupy the controllability-sufficient region of the phase diagram, consistent with dynamics that are effectively static or smoothly varying over the evaluation horizon.

Macro-finance (0.09) and democracy (0.04) exhibit larger departures, suggesting richer regime structure. The magnitude of the spread under the realized baseline is modest (0.01–0.09), but this is itself informative: the measure remains close to controllability where the phase diagram predicts it should and departs only on systems displaying stronger dynamical heterogeneity. The separation between these two regime-changing panels and the three near-zero physical panels holds across every seed of the retraining ensemble, rather than arising from a single fit. A diagnostic of realized regime structure finds highly persistent but sign-stable drivers in macro-finance and partial sign reversal in democracy, corresponding to two of the departure mechanisms identified in Section IX-A (persistent reroute and sign reversal).

The pooled-baseline comparison, departure from a single mean-state linearization, is the more permissive of the two, but it is markedly less stable across retrains on every panel: pooled departures vary widely (for example, roughly 0.02–0.33 on economic development), so we do not report pooled point estimates and instead lead on the realized baseline throughout. This instability is itself consistent with the hierarchy of approximations from Section IX-A: a single linearization is a weak summary of trajectory structure, so its agreement with E_j is both smaller and more fragile than that of the averaged-Jacobian baseline, which remains strongly and stably aligned with E_j ($\rho \approx 0.93$ – 0.98 across seeds on the democracy panel).

Taken together, these results support a practical decision rule. Emergent contribution provides the greatest value on

systems that depart from the controllability-sufficient corner of the phase diagram, and a system’s realized departure offers an empirical diagnostic of where it lies.

b) One domain in depth - a robust variance-leverage dissociation: We examine the V-Dem democracy panel as a worked example using a twenty-seed retraining ensemble (validation MSE 0.043 ± 0.0003). Dynamical leverage does not merely restate how much a component moves. Across components, E_j is essentially uncorrelated with within-country temporal variance (Spearman 0.03). By contrast, E_j correlates substantially with one-step influence (out-strength 0.80) and two-step reach (0.78).

The dissociation is visible in specific components. *Elected officials* has the highest within-country variance of all sixteen indicators yet consistently appears in the bottom leverage tier (typically rank 14 across seeds). Likewise, *suffrage* combines the second-highest variance with bottom-tier leverage (rank 16 in the modal seed). Both variables move substantially, but their movement does not propagate widely through the estimated system.

These conclusions are robust to estimation noise. Across the twenty retrained models, the highest- and lowest-leverage components remain sharply identified: freedom of association and freedom of expression occupy the top two ranks in every seed (each spanning ranks 1–3), while suffrage and direct vote occupy the bottom two (ranks 14–16). Individual liberty and elected officials remain consistently within the top and bottom tiers, respectively, although their exact ranks vary. Uncertainty is concentrated in the middle of the ordering, where the remaining ten components reshuffle freely (mean pairwise Spearman 0.85). The practical implication is that leverage tiers are reliably identified, whereas fine distinctions among middle-ranked components are not.

XI. DISCUSSION AND CONCLUSION

We introduced a measure of finite-horizon dynamical leverage for estimated nonlinear, time-varying systems, showed that it reduces exactly to average controllability in the linear time-invariant limit, and characterized the conditions under which the two measures diverge. Across synthetic systems with known ground truth and across five empirical domains, emergent contribution captures structure that neither static controllability nor variance-based summaries recover.

a) What the measure is and is not: Emergent contribution measures dynamical leverage, not importance: the claim is descriptive, that a component has a particular leverage within the estimated system, and any normative interpretation of that leverage requires a separate domain-specific argument.

b) Limitations and extensions: The measure is finite-horizon by design. For systems near or beyond marginal stability, impulse-response energy grows with the evaluation horizon, making the choice of T an explicit modeling decision that must be stated and held fixed when comparing results. As a functional of estimated Jacobians, E_j also inherits estimation uncertainty; the retraining ensemble used for the democracy panel illustrates one approach to quantifying that uncertainty.

Finally, several natural extensions remain open, including modal-controllability analogues and definitions of contribution relative to a basin of attraction in multi-equilibrium systems.

c) Conclusion: We defined a finite-horizon measure of node-level contribution for estimated nonlinear, time-varying systems, proved its exact reduction to average controllability in the linear time-invariant limit, and characterized the conditions under which the two measures diverge. Departures emerge under persistent regime change, with sign reversal the strongest case. In those settings, emergent contribution provides a practical, estimator-agnostic measure that recovers the trusted linear answer when appropriate and extends it when the dynamics demand more.

REFERENCES

- [1] Y.-Y. Liu, J.-J. Slotine, and A.-L. Barabási, “Controllability of complex networks,” *Nature*, vol. 473, no. 7346, pp. 167–173, 2011.
- [2] F. Pasqualetti, S. Zampieri, and F. Bullo, “Controllability metrics, limitations and algorithms for complex networks,” *IEEE Transactions on Control of Network Systems*, vol. 1, no. 1, pp. 40–52, 2014.
- [3] L. C. Freeman, “Centrality in social networks: Conceptual clarification,” *Social Networks*, vol. 1, no. 3, pp. 215–239, 1978.
- [4] L. Page, S. Brin, R. Motwani, and T. Winograd, “The pagerank citation ranking: Bringing order to the web,” Stanford InfoLab, Tech. Rep., 1999.
- [5] D. Borsboom and A. O. J. Cramer, “Network analysis: An integrative approach to the structure of psychopathology,” *Annual Review of Clinical Psychology*, vol. 9, no. 1, pp. 91–121, 2013.
- [6] S. Epskamp, D. Borsboom, and E. I. Fried, “Estimating psychological networks and their accuracy: A tutorial paper,” *Behavior Research Methods*, vol. 50, no. 1, pp. 195–212, 2018.
- [7] M. N. Hallquist, A. G. C. Wright, and P. C. M. Molenaar, “Problems with centrality measures in psychopathology symptom networks: Why network psychometrics cannot escape psychometric theory,” *Multivariate Behavioral Research*, vol. 56, no. 2, pp. 199–223, 2021.
- [8] S. Gu, F. Pasqualetti, M. Cieslak, Q. K. Telesford, A. B. Yu, A. E. Kahn, J. D. Medaglia, J. M. Vettel, M. B. Miller, S. T. Grafton, and D. S. Bassett, “Controllability of structural brain networks,” *Nature Communications*, vol. 6, p. 8414, 2015.
- [9] R. T. Q. Chen, Y. Rubanova, J. Bettencourt, and D. Duvenaud, “Neural ordinary differential equations,” in *Advances in Neural Information Processing Systems (NeurIPS)*, vol. 31, 2018, pp. 6572–6583.
- [10] A. Tank, I. Covert, N. Foti, A. Shojaie, and E. B. Fox, “Neural Granger causality,” *IEEE Transactions on Pattern Analysis and Machine Intelligence*, vol. 44, no. 8, pp. 4267–4279, 2022.
- [11] B. Bussmann, J. Nys, and S. Latré, “Neural additive vector autoregression models for causal discovery in time series,” in *Discovery Science (DS 2021)*, ser. Lecture Notes in Computer Science, vol. 12986. Springer, 2021, pp. 446–460.
- [12] S. Lall, J. E. Marsden, and S. Glavaški, “A subspace approach to balanced truncation for model reduction of nonlinear control systems,” *International Journal of Robust and Nonlinear Control*, vol. 12, no. 6, pp. 519–535, 2002.
- [13] M. O. Williams, I. G. Kevrekidis, and C. W. Rowley, “A data-driven approximation of the Koopman operator: Extending dynamic mode decomposition,” *Journal of Nonlinear Science*, vol. 25, no. 6, pp. 1307–1346, 2015.
- [14] H. K. Khalil, *Nonlinear Systems*, 3rd ed. Prentice Hall, 2002.
- [15] M. Sundararajan, A. Taly, and Q. Yan, “Axiomatic attribution for deep networks,” in *Proceedings of the 34th International Conference on Machine Learning (ICML)*, ser. PMLR, vol. 70, 2017, pp. 3319–3328.
- [16] D. Kempe, J. Kleinberg, and É. Tardos, “Maximizing the spread of influence through a social network,” in *Proceedings of the 9th ACM SIGKDD International Conference on Knowledge Discovery and Data Mining (KDD)*, 2003, pp. 137–146.
- [17] M. Coppedge, J. Gerring, C. H. Knutsen, S. I. Lindberg, J. Teorell *et al.*, “V-Dem country-year dataset v15,” Varieties of Democracy (V-Dem) Project, 2025.
- [18] World Bank, “World development indicators,” World Bank, Washington, DC, 2024.

- [19] K. Müller, C. Xu, M. Lehib, and Z. Chen, "The global macro database: A new international macroeconomic dataset," National Bureau of Economic Research, Working Paper 33714, April 2025.
- [20] B. Son, Y. Lee, S. Park, and J. Lee, "Forecasting global stock market volatility: The impact of volatility spillover index in spatial-temporal graph-based model," *Journal of Forecasting*, vol. 42, no. 7, pp. 1539–1559, 2023.
- [21] S. Zhang, B. Guo, A. Dong, J. He, Z. Xu, and S. X. Chen, "Cautionary tales on air-quality improvement in Beijing," *Proceedings of the Royal Society A*, vol. 473, no. 2205, p. 20170457, 2017.